Journal of the Optical Society of Korea, Vol. 7, No. 3, September 2003, pp. 180-187

Effect of a Conductor Cladding on a Dielectric Slab for Coupling with a Side-polished Fiber

Kwang-Hee Kwon* and Jae-Won Song

Dept. of Electronics Engineering, Kyungpook National University, Daegu 702-701, KOREA

(Received February 18, 2003)

A theoretical presentation by using a three-dimensional finite difference beam propagating method (3-D FD-BPM) for the evanescent coupling is offered with respect to the refractive indexes between a side-polished optical fiber and an infinitely planar waveguide with a conductor cladding (PWGCC). The PWG is suspended at a constant distance from an unclad fiber core and attached with a perfect conductor (PEC) on one side. The coupling and propagation of light are found to depend on both the relationship between the refractive index values of two structures and the configuration of the side-polished fiber used in the PWGCC. The spreading of light in the unconfined direction of a PWGCC is presented with the distribution of electric fields in xy - plane and the absolute amplitude of electric fields along the x and y axis. The power of the light propagation in a fiber decreases exponentially along the fiber axis as it is transferred to the PWGCC, where it is carried away.

OCIS code : 250.0250.

I. INTRODUCTION

The exchange of energy between an optical fiber and a PWG placed alongside in close proximity has attracted much attention over the years due to its challenging intrinsic complexity and potential application in many fields. A side-polished fiber-slab waveguide structure, consisting of a single-mode optical D-shaped fiber with a flat cladding surface attached to the PWG overlay, has also been used in channel-dropping filters [1], polarizers [2], intensity modulators [3], [4] and sensors [5]. For example, Marcuse [6] and Shu Zheng [7] developed a theoretical analysis using CMT as a single-mode fiber-optic polished coupler with a PWG layer formed by optical glue between the two half-blocks of the coupler. However, the coupling between a fiber and a PWGCC has not yet been investigated. Therefore, the current study investigates a composite fiber-slab structure with a conducting surface attached to one side of a PWG by using a 3-D FD-BPM analysis, thereby asymmetrically extending the analysis by Shu Zheng [7]. To analyze a composite fiber-slab structure without a conductor cladding, Even though Marcuse [6] and Shu Zheng [7] assumed that a pair of hypothetical walls were also imposed at a significant distance along the y -axis, a 3-D FD-BPM analysis was conducted for the coupling between a side-polished fiber and a PWGCC without the hypothetical walls. So the current authors consider that this 3-D FD-BPM analysis for this system is close to a real situation. Plus it is also assumed that the combined system of a fiber and a PWGCC can be regarded as a ridge waveguide, as in references [6], [7], and [8]. According to these references, when the fiber mode is essentially synchronous with the ridge mode, considerable beating occurs initially between the guided and unguided compound modes of the system until a guided ridge mode is established through the PWGCC. When a fiber mode is infinitely coupled, many of the PWGCC modes suffer coupling-induced attenuation. Plus, when the fiber propagation constant lies deep within the range of the propagation constants of the continuum slab modes in the PWGCC, an exponential decay of the light carried in the fiber is observed. Accordingly, to represent the effect of coupling between the two structures, the amplitude of the electric field in the propagating direction for the coupling of a composite side-polished fiber and PWGCC is presented by using a 3-D FD-BPM analysis and compared with it of a composite-polished fiber and PWG without a conductor cladding.

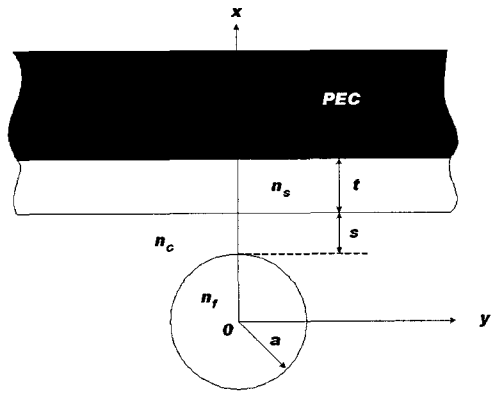

FIG. 1. Cross-sectional view of a planar wave guide under a perfect conductor(PWGCC) suspended above a fiber.

II. A 3D FD-BPM FOR A COMPOSITE FIBER-PWGCC COUPLER

Longitudinal and cross-sectional views of the distributed single-mode fiber-to PWGCC coupler are presented in Fig. 1. The Maxwell's equations written for a source and charge free are combined first. The scalar approximation is applied whenever all the refractive index differences remain small [9]. Therefore, based on the scalar approximation the scalar wave equation is as follows:

$$\nabla^2 E(x,y,z) + k^2 n^2(x,y,z) E(x,y,z) = \nabla(\nabla \cdot E(x,y,z)) \tag{1}$$

where E is the transverse electric field of a fiber-PWGCC system, $\nabla^2 = \frac{\partial^2}{\partial x^2} + \frac{\partial^2}{\partial y^2} + \frac{\partial^2}{\partial z^2}$, k is the wave number in free space, and $n(x,y,z)$ defines the local refractive index. As shown in Fig. 1, the index profiles of a unperturbed fiber and a PWGCC are

$$n(x,y,z) = \left\{ \begin{array}{ll} n_f & \text{for } x^2+y^2 \le a^2 \\ n_s & \text{for } a+s \le x \le a+s+t \\ n_c & \text{elsewhere} \end{array} \right\} \text{at any } z \tag{2}$$

Where a is the radius of a fiber core, t is the thickness of a PWGCC, s is the distance between a fiber and a PWGCC in (2) and (3), n_f is the refractive index of a fiber, n_c is the refractive index of a cladding, and n_s is the refractive index of a PWGCC in (2). The current study is only restricted to cases of a single LP_{01} mode of guided fiber. If z is associated to the propagation direction, one can write any component $E(x,y,z)$ as a product of a rapidly varying propagation term $(e^{-jkn_c z})$ and a slowly varying one $F_i(x,y,z)$:

$$E_i(x,y,z) = F_i(x,y,z) e^{-jkn_c z} \tag{3}$$

Making use of the well known slowly varying envelope approximation (SVEA), i.e., assuming that the following condition holds:

$$\left| \frac{\partial^2 F_i}{\partial z^2} \right| \ll 2kn(x,y,z) \left| \frac{\partial F_i}{\partial z} \right| \tag{4}$$

The 3-D paraxial scalar wave equation is as follows:

$$\begin{aligned} \frac{\partial F_i}{\partial z} = & -\frac{1}{2kn_c} \nabla_t^2 F_i - \alpha(x,y,z) F_i \\ & - j\frac{k}{2n_c} \left[n^2(x,y,z) - n_c^2 \right] F_i \end{aligned} \tag{5}$$

Where $\alpha(x,y,z)$, a loss or gain term, is added and $\nabla_t^2 = \frac{\partial^2}{\partial x^2} + \frac{\partial^2}{\partial y^2}$. To solve Eq. (5), a 3D FD-BPM has been adopted: the continuous space is discretized into a lattice structure defined in the computational region using a Δx, Δy, Δz mesh and all the differential operators are replaced by their corresponding finite-difference ones. The differential operators are then substituted by difference ones yield a set of linear algebraic equations, in which the three field components at the generic propagation step m can be expressed in terms of the field components at the previous one. The electric field at the grid point of $x = i\Delta x$, $y = l\Delta y$ and $z = m\Delta z$ is expressed by

$$F(i\Delta x, l\Delta y, m\Delta z) = F_{i,l}^m \tag{6}$$

Using this notation for the field, Eq. (5) is approximated by the finite difference form as

$$\begin{aligned} A(F_{i,l}^{m+1} - F_{i,l}^m) = & \frac{F_{i-1,l}^m - 2F_{i,l}^m + F_{i+1,l}^m + F_{i-1,l}^{m+1} - 2F_{i,l}^{m+1} + F_{i+1,l}^{m+1}}{2(\Delta x)^2} \\ & + \frac{F_{i,l-1}^m - 2F_{i,l}^m + F_{i,l+1}^m + F_{i,l-1}^{m+1} - 2F_{i,l}^{m+1} + F_{i,l+1}^{m+1}}{2(\Delta y)^2} + B(F_{i,l}^{m+1} + F_{i,l}^m) \end{aligned} \tag{7}$$

Where $A = \frac{j2kn_c}{\Delta z}$, $B = -jkn_c\alpha\left(i,l,m+\frac{1}{2}\right) + \frac{k^2}{2}\left[n^2\left(i,l,m+\frac{1}{2}\right) - n_c^2\right]$. This finite difference eq. (7) for the three-dimensional problem is not a tridiagonal equation as in the two-dimensional problems. Therefore, generally an inverse matrix operation is required. However, the following approximate solution

method, which is called alternating-direction implicit finite difference method (ADIFDM) [10], can greatly simplify the calculation procedures for Eq. (7). The solution in Eq. (7) can be found when field initial values are defined. Plus, should radiation occur, it must be completely absorbed at the boundary of open structure, as usually dielectric ones are, to avoid unphysical numerical reflections into the computational domain, leading to meaningless results. Accurate boundary conditions is then required. So the perfectly matched layer (PML) boundary [11], [12] conditions is used instead of the transparent boundary conditions (TBC) [13], which is not reliable in 3-D cases.

III. NUMERICAL RESULTS AND DISCUSSION

Numerical results for coupling with a side-polished fiber are presented for the PWGCC that is a special asymmetric case in reference [7]. All the optical and structural parameters are defined as in reference [7], except for the PEC attached to the PWG. The investigation of the structure is carried out using a single-mode fiber (SMF) with the following parameters: light wavelength $\lambda = 1.3\mu m$, fiber core radius $a = 2.5\mu m$, thickness of a PWGCC $t = 3\mu m$, refractive index of fiber cladding $n_c = 1.46$ and refractive index of a PWGCC $n_s = 1.4745$. The minimal distance between a fiber core and a PWGCC is called the polishing depth and denoted by s. The thickness of a PWGCC is choose to propagate at least the lowest mode among the guiding trapped wave modes [14]. The value of the refractive index of the fiber core n_f varies around that of the PWGCC, i.e. $n_f > n_s$, $n_f = n_s$, and $n_f < n_s$, respectively. To study the couple mode equation between the side-polished fiber and each PWG by using a 3-D FD-BPM analysis, it is also assumed that only the LP_{01} mode is initially launched through the fiber at $z = 0$ starting at any

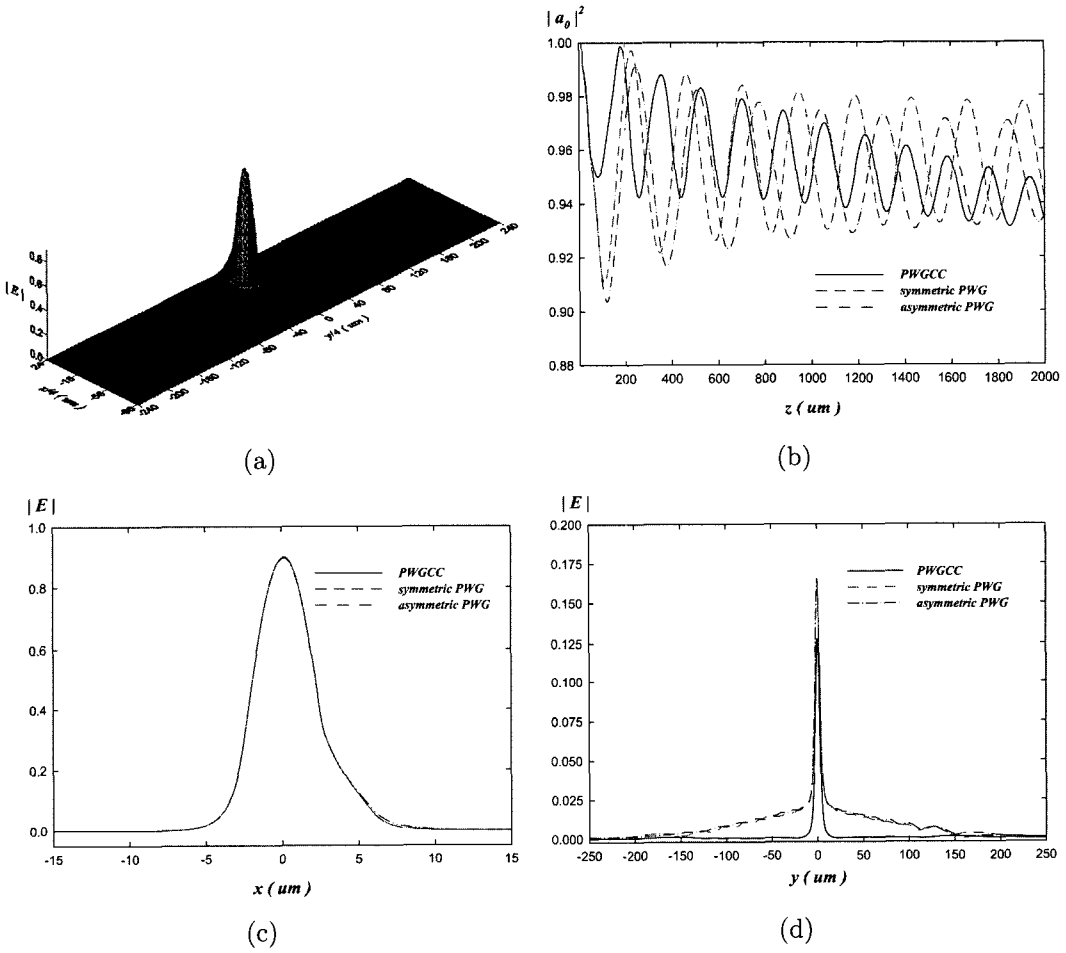

FIG. 2. Field $|E|$ for fiber-each PWG at $z = 2000\mu m$ when $\Delta_f = 0.015$ and $s = 0.5\mu m$. (a) Field $|E|$ distribution in xy - plane (b) Absolute squares of excitation coefficients for fiber mode as function of light propagation distance z in fiber. (c) Field $|E|$ for fiber-each PWG as function of x in plane $y = 0$. (d) Field $|E|$ for fiber-each PWG as function of y in each PWG.

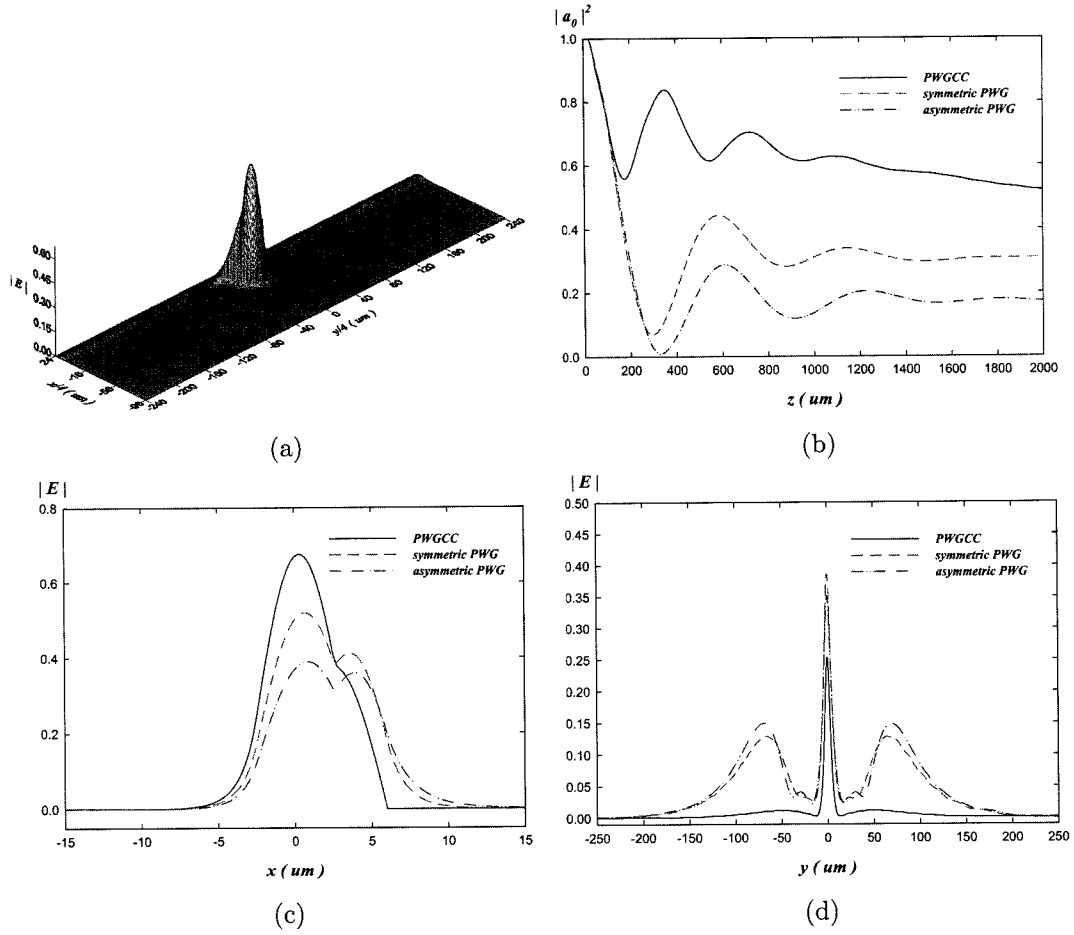

FIG. 3. Field $|E|$ for fiber-each PWG at $z = 2000\mu m$ when $\Delta_f = 0.01077$ and $s = 0.5\mu m$. (a) Field $|E|$ distribution in xy - plane (b) Absolute squares of excitation coefficients of fiber mode as function of light propagation distance z in fiber. (c) Field $|E|$ of fiber-each PWG as function of x in plane $y = 0$. (d) Field $|E|$ of fiber-each PWG as function of y in each PWG.

$z = 0$. When a 3-D FD-BPM analysis is applied to a composite fiber-each PWG system, the width of a 3-D FD-BPM analysis is $60\mu m$ in the x - axis direction, $500\mu m$ in the y - axis direction and the number of divisions is $\Delta_x = \Delta_y = 0.25\mu m$. The calculation step along the z direction is $\Delta_z = 0.5\mu m$. Plus it is assumed that the refractive index for the upper region of the asymmetric PWG is 1.4565 to simulate a 3-D FD-BPM analysis. Fig. 2(a) indicates the field $|E|$ distribution in the xy - plane at $z = 2000\mu m$ in the case of $\Delta_f = 0.015$ and $s = 0.5\mu m$ according to a 3-D FD-BPM analysis. Fig. 2(b) shows that, when $n_f > n_s$, the coupling between a fiber and each PWG is ineffective regardless of the kind of PWG, only a fraction of the launched power in a fiber fluctuates between a fiber and each PWG, and the light power remains largely in the fiber. In the absence of coupling, the fiber mode is not in phase synchronism with any PWGCC modes and a little power is coupled from a fiber to a PWGCC. Fig. 2(c) shows the field $|E|$ for a fiber-each PWG as a function of x in plane $y = 0$. As shown in Fig. 2(c), the form of the field $|E|$ in the fiber is not symmetric and there are some deformations of the symmetric mode of the isolated fiber due to minimal coupling with the PWGCC. Fig. 2(d) shows the field $|E|$ for the fiber-each PWG as a function of y in each PWG. The field $|E|$ in a PWGCC is concentrated near $y = 0$ for the PWG without a conductor cladding, even though the amplitude of the field $|E|$ in a PWGCC was slightly smaller than that of each PWG without a conductor cladding. Fig. 3(a) indicates the field $|E|$ distribution in the xy - plane at $z = 2000\mu m$ when $\Delta_f = 0.01077$ and $s = 0.5\mu m$ according to a 3-D FD-BPM analysis. Fig. 3(b) shows that, when n_f is similar or slightly larger than n_s, the coupling between a fiber and each PWG without a conductor cladding is more effective than with a PWGCC, plus a lot of the power launched in the fiber fluctuates between a fiber and each PWG. But a little of the light power in the PWG without a conductor cladding remains in the fiber, yet a lot of the light power in the PWGCC remains in the fiber. So, lowering the value

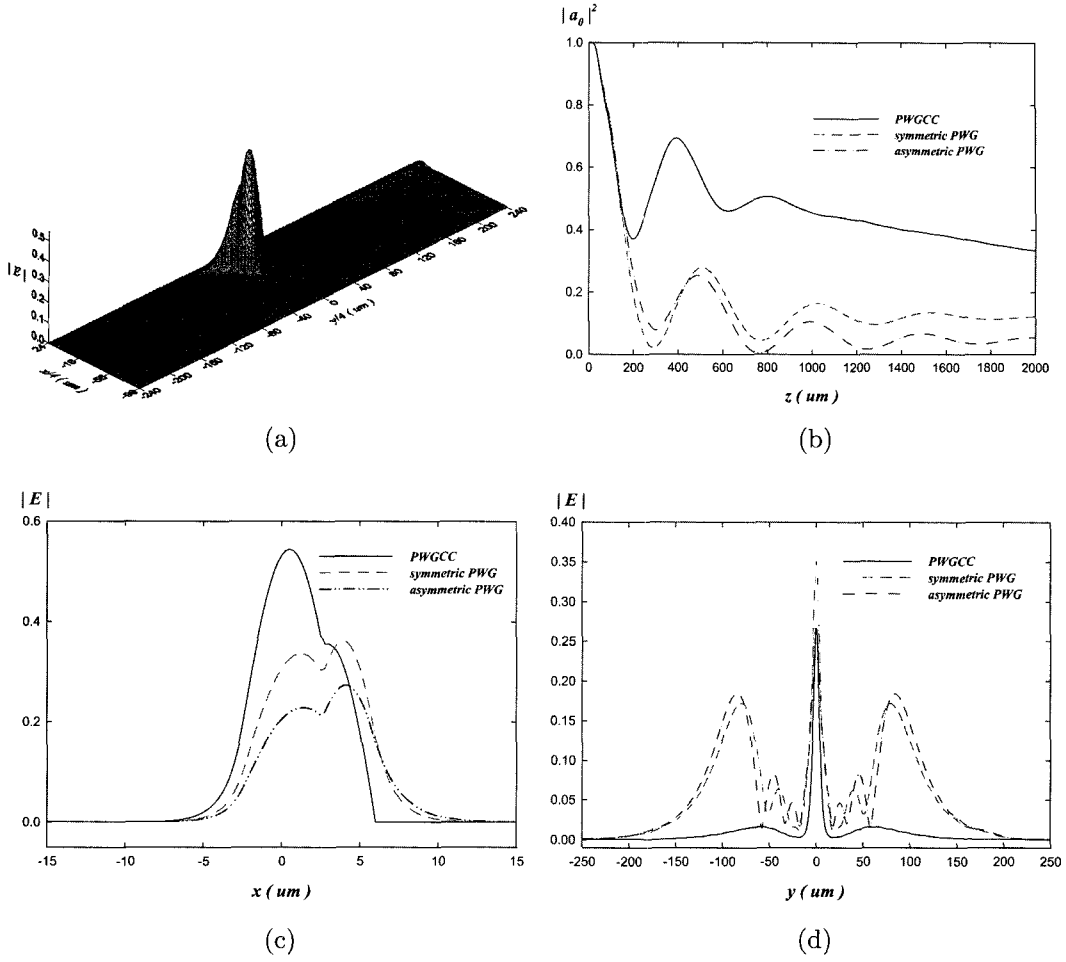

FIG. 4. Field $|E|$ for fiber-each PWG at $z = 2000\mu m$ when $\Delta_f = 0.01$ and $s = 0.5\mu m$. (a) Field $|E|$ distribution in xy - plane (b) Absolute squares of excitation coefficients of fiber mode as function of light propagation distance z in fiber. (c) Field $|E|$ of fiber-each PWG as function of x in plane $y = 0$. (d) Field $|E|$ of fiber-each PWG as function of y in each PWG.

n_f generally causes the power oscillation to decay slightly and increases the rate of decay of the power beating, thereby transferring power from a fiber to each PWG due to the reduced phase mismatch. Fig. 3(c) shows the field $|E|$ of a fiber-each PWG as a function of x in plane $y = 0$. As shown in Fig. 3(c), the light power in a fiber is mostly transferred to the PWG without a conductor cladding, whereas most of the light power in a PWGCC remains in the fiber. Fig. 3(d) shows the field $|E|$ of the fiber-each PWG as a function of y in each PWG, and a little of the field $|E|$ in the case of a PWG without a conductor cladding is propagated along the y - axis. The field $|E|$ in the PWGCC is concentrated near $y = 0$, yet the amplitude of the field $|E|$ in the PWGCC is slightly smaller than that of the PWG without a conductor cladding. Fig. 4(a) indicates the field $|E|$ distribution in the xy - plane at $z = 2000\mu m$ when $\Delta_f = 0.01$ and $s = 0.5\mu m$ according to the 3-D FD-BPM analysis and Fig. 4(b) shows that, when n_f is the same as n_s, the amount of power coupled out of the fiber is strongly dependent, plus the power beating and light power transferred to a PWGCC becomes increasingly larger. Most of the power launched in a fiber fluctuates between a fiber and each PWG, and only a little of the light power in each PWG without a conductor cladding remains in the fiber, whereas most of the light power in the PWGCC remains in the fiber. Fig. 4(c) shows the field $|E|$ of the fiber-each PWG as a function of x in plane $y = 0$. As shown in fig. 4(c), large humps appear in the field around the position of each PWG. But most of the light power in the fiber is transferred to each PWG without a conductor cladding, although a lot of the light power remains in the fiber. Based in Fig. 4(c), the variation of the refractive index n_f causes more deformation of the pure fiber mode and the large fractions of mode power are gradually transferred to each PWG from the fiber. Fig. 4(d) shows the field $|E|$ of the fiber-each PWG as a function of y in each PWG. As shown in Fig. 4(d), a little of the field $|E|$ in each PWG without a conductor cladding is propagated along the y - axis, whereas a lot of the

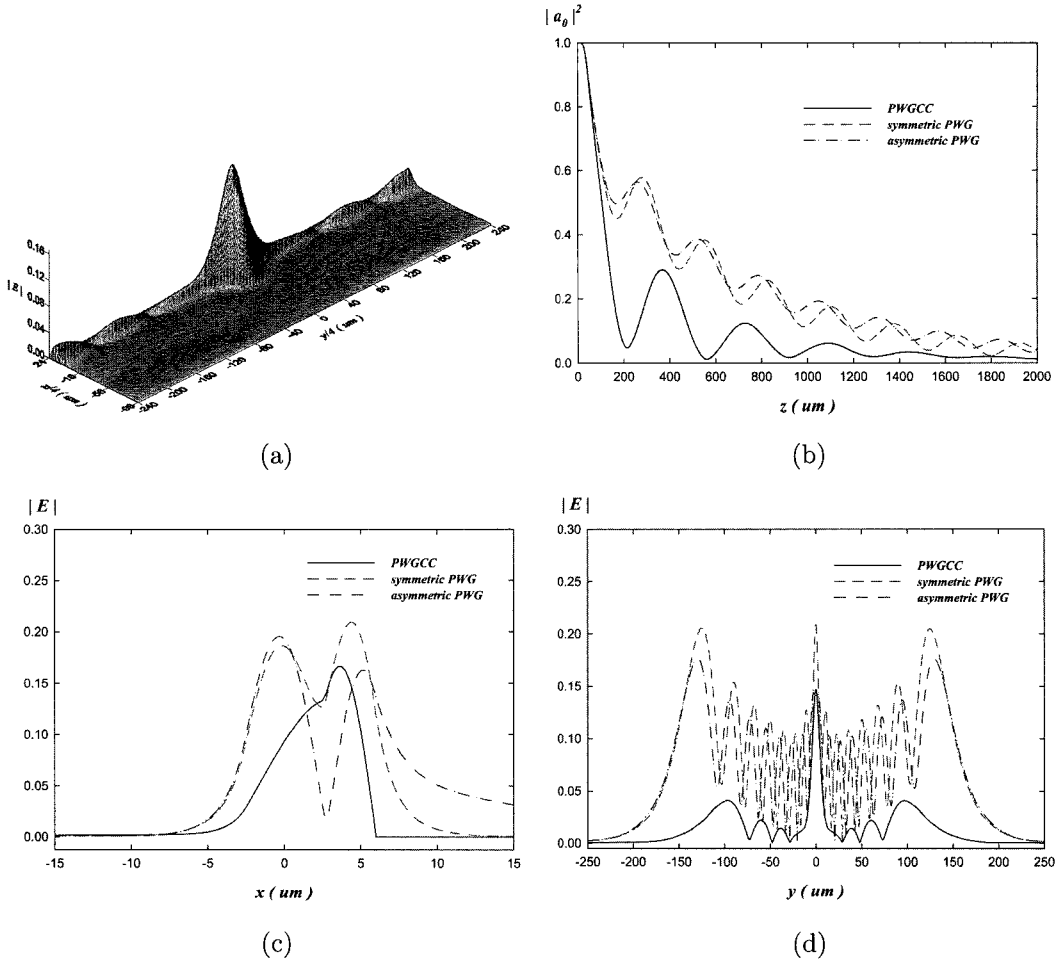

FIG. 5. Field $|E|$ for fiber-each PWG at $z = 2000\mu m$ when $\Delta_f = 0.0075$ and $s = 0.5\mu m$. (a) Field $|E|$ distribution in xy - plane (b) Absolute squares of excitation coefficients of fiber mode as function of light propagation distance z in fiber. (c) Field $|E|$ of fiber-each PWG as function of x in plane $y = 0$. (d) Field $|E|$ of fiber-each PWG as function of y in each PWG.

field $|E|$ is concentrated near $y = 0$ in the PWGCC, although a fraction of the field $|E|$ is propagated the along y - axis and the amplitude of the field $|E|$ is smaller than that of the PWG without a conductor cladding. Fig. 5(a) indicates the field $|E|$ distribution in the xy - plane at $z = 2000\mu m$ when $\Delta_f = 0.0075$ and $s = 0.5\mu m$ according to the 3-D FD-BPM analysis and Fig. 5(b) shows that, when the value of n_f is less than that of n_s, the fiber mode decays in such a way that the smaller the value of n_f relative to the value of n_s, the stronger the coupling to each PWG, as shown in Fig. 5(b). Thus, the power oscillates with a high strength and dies out. Since the rate of decay of the power beating and power is substantially transferred from a fiber to each PWG, the absolute square of the fiber mode amplitude $|a_\theta|^2$ reduces to nearly zero beyond a certain propagation distance(typically $2000\mu m$) from the initial value of $|a_\theta|^2$ at $z = 0$. Fig. 5(c) shows the field $|E|$ of the fiber-each PWG as a function of x in plane $y = 0$. As shown in Fig. 5(c), nearly all the light power in the fiber is transferred to each PWG. Fig. 5(d) shows the field $|E|$ of the fiber-each PWG as a function of y in each PWG. A lot of the field $|E|$ in each PWG without a conductor cladding fluctuates and is propagated along the y - axis, whereas most of the field $|E|$ in a PWGCC remains near $y = 0$, although a small part of the field $|E|$ fluctuates and is propagated along the y - axis. The peak values of the ridge-mode fields are dependent on the relative values of n_f, and the rate of the power transferred to each PWG is generally slightly higher. According to Figs. 2(a)- 5(d), the simulation results by the 3-D FD-BPM analysis matches very well with the physical phenomena for the symmetric and asymmetric PWG reported in references [6] and [7] and are presented the peculiar properties of the PWGCC for each PWG without a conductor cladding.

As shown in Fig. 6(a), the power beating and power transferred to the PWGCC became larger as the distance between the structures became smaller. The absolute square of the fiber mode amplitude $|a_\theta|^2$ was represented for s according to the refractive index of

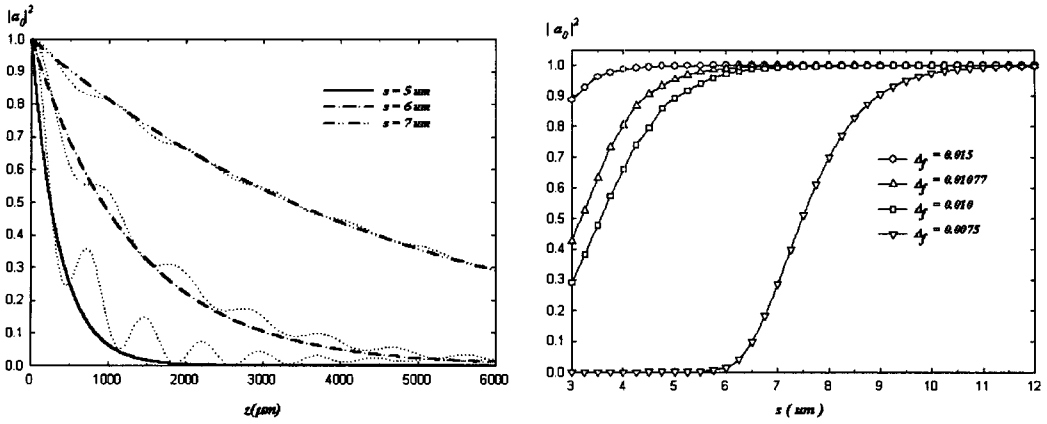

FIG. 6. Absolute squares of excitation coefficients of fiber mode as function of light propagation distance z in fiber about TE mode in the PWGCC. (a) fiber-mode loss to PWGCC, namely exponential curves for s, and (b) absolute square of the fiber mode amplitude $|a_\theta|^2$ for s according to the refractive index of the fiber.

the fiber in Fig. 6(b). Fig. 6(b) shows that, when the refractive index of the fiber is larger than that of the PWGCC, only a fraction of the light power in the fiber is transferred to the PWGCC, even though the distance between the fiber and the PWGCC was slightly smaller. Yet, when the refractive index of the fiber was smaller than that of the PWGCC, a lot of the light power in the fiber was transferred to the PWGCC, even though the distance s was slightly larger. Therefore, Figs. 6(a) and (b) show that the distance between both structures, s, also affects the sensitivity of the coupling of the side-polished fiber and the PWGCC as well as the difference in the refractive index for each waveguides. So the light transfer between the fiber and the PWGCC was found to depend strongly on the relationship between their propagation constants $\beta_{f\theta}$ and β_s. When β_s was considerably larger than $\beta_{f\theta}$, the PWGCC also acted as a sink for the optical power in the fiber, so that the total power launched initially into the fiber was spread out laterally in the PWGCC. A compound equation was also used to represent the transverse electric field for the propagating direction at $y = 0$ and Newton-Raphson's method used to obtain the eigenvalue from the compound equations [15]. These modes exhibited a common propagation constant for the entire system and a stationary power distribution beyond a certain distance of propagation.

IV. CONCLUSION

In conclusion, an analysis of a composite fiber-PWGCC was conducted and the drain of optical power from a fiber to a PWGCC was shown to depend on a combination of the relative values of n_f, n_s. The properties of the coupling between a side-polished fiber and a PWGCC for the ridge modes were presented based on a 3-D FD-BPM analysis for this system. The exchange of energy between a fiber and a PWGCC was visualized by comparing the light intensity at different cross sections of a fiber-slab combination along the propagation direction and the characteristics of a fiber and a PWGCC mode-coupling presented, especially the features of the power oscillations and beatings. As shown in each figure, when n_s was lower than n_f, the light was generally well confined within the fiber core. However, as soon as n_s approached or became higher than n_f, the mode beating, decay, and amount of the power transferred could be readily tuned by a small variation in the value n_f. When the refractive index of a fiber was smaller than that of a PWGCC, the power beating and light power also became increasingly larger. Finally the proposed structure consisting of a fiber and a PWGCC is very different from those of conventional directional couplers as regards the aspect of light power exchange. The proposed process provides a loss mechanism that is describable in terms of a loss coefficient. The PWGCC also tended to act as a power sink for a fiber as in a system with a PWG without a conductor cladding. The proposed system can also be used to tap light out of a fiber without the need for a critical length adjustment of the coupler based on the properties of a PWGCC, where most of the compound modes spread out over the entire PWGCC, as in a system with a PWG without a conductor cladding. Given a sufficient length and width, the light transfers from a fiber to a PWGCC without ever coming back. This may also be an efficient mechanism for exciting a PWGCC for certain specialized integrated optic applications. So the current authors

believe that the proposed system may be useful in various optic applications and fields that utilize the loss of light power.

*Corresponding author : tree@palgong.knu.ac.kr

REFERENCES

[1] C. A. Millar, M. C. Brierley, and S. R. Mallinson, "Exposed-core single-mode-fiber channel-dropping filter using a high-index overlay waveguide," *Opt. Lett.*, vol. 12, pp. 284-286, 1987.

[2] W. Johnstone, G. Stewart, B. Culshaw, and T. Hart, "Fiber-optic polarisers and polarising couplers," *Electron. Lett.*, vol. 24, pp. 866-868, 1988.

[3] W. Johnstone, S. Murray, G. Thursby, M. Gill, A. McDonach, D. Moodie, and B. Culshaw, "Fiber optical modulators using active multimode waveguide overlays," *Electron. Lett.*, vol. 27, pp. 894-896, 1991.

[4] G. Fawcett, W. Johnstone, I. Andonovic, D. J. Bone, G. Harvey, N. Carter, and T. G. Ryan, "In-line fiber-optic intensity modulator using electro-optic polymer," *Electron. Lett.*, vol. 28, pp. 985-986, 1992.

[5] G. Thursby, W. Johnstone, K. McCallion, D. Moodie, and B. Culshaw, "A novel fiber refractive index sensor using resonance shift phenomena," in *Proc. 8th Optical Fiber Sensors Conf.*, Monterey, CA, pp. 197-200, 1992.

[6] D. Marcuse, "Investigation of coupling between a fiber and an infinite slab," *J. Lightwave Technol.*, vol. 7, pp. 122-130, 1989.

[7] Shu Zheng, Le N. Binh, and George P. Simon. "Light coupling and propagation in composite optical fiber-slab waveguides," *J. Lightwave Technol.*, vol. 13, No. 2, pp. 244-250, 1995.

[8] E. A. J. Marcatili, "Slab-coupled waveguides." *Bell Syst. Tech. J.*, vol. 53, pp. 645-674, 1974.

[9] D. Gloge, "Weakly guiding fibers," *Appl. Opt.*, vol. 10, pp. 2252-2258, 1971.

[10] W. H. Press, B. P. Flannery, S. A. Teukolsky, and W. T. Vettering, *Numerical Recipes: The Art of Scientific Computing* (Cambridge University Press, Cambridge, UK, 1986).

[11] J. Berenger, "A perfectly matched layer for the absorption of electromagnetic waves," *J. Computational Phys.*, vol. 114, no. 1, pp. 185-200, 1994.

[12] W. P. Huang, C. L. Xu, W. Lui, and K. Yokoyama, "The perfectly matched layer (PML) boundary condition for the beam propagation method," *IEEE Photon. Technol. Lett.*, vol. 8, pp. 649-651, 1996.

[13] G. R. Hadley, "Transparent boundary conditions for the beam propagation method," *Opt. Lett.*, vol. 16, no. 9, pp. 624-626, 1991.

[14] Akira Ishimaru, *Electromagnetic wave Propagation, radiation, and scattering* (Englewood Cliffs, N.J.: Prentice-Hall Inc., 1991).

[15] Kwang-Hee Kwon, Jae-Won Song, and Jeong-Hoon Kim, "The analysis of Light Coupling and Propagation for a Composite Fiber-Dielectric Slab with a Conductor Cladding," *Journal of the Optical Society of Korea*, vol. 7, No. 1, pp. 20-27, 2003.